https://doi.org/10.5194/nhess-2020-198
Preprint. Discussion started: 7 July 2020

Natural Hazards and Earth System Sciences
Discussions

Wave climate and storm activity in the Kara sea

Stanislav Myslenkov[1,2,3], Vladimir Platonov[1], Alexander Kislov[1], Ksenia Silvestrova[2], Igor Medvedev[2,4]

[1]Lomonosov Moscow State University, 119991, Moscow, Russia

[2]Shirshov Institute of Oceanology RAS, 117997, Moscow, Russia

[3]Hydrometeorological Research Centre of the Russian Federation, 123242, Moscow, Russia

[4]Fedorov Institute of Applied Geophysics, 129128, Moscow, Russia

Correspondence to: Stanislav Myslenkov (stasocean@gmail.com)

Abstract. Recurrence of extreme wind waves in the Kara Sea strongly influences the Arctic climate change. The paper presents the analysis of wave climate and storm activity in the Kara Sea based on the results of numerical modeling. A third-generation wave model WaveWatchIII is used to reconstruct wind wave fields on an unstructured grid with a spatial resolution of 15–20 km for the period from 1979 to 2017.

The mean and maximum wave heights, wavelengths and periods are calculated. The maximum significant wave height (SWH) for the whole period amounts to 9.9 m. The average long-term SWH for the ice-free period does not exceed 1.3 m. The seasonal variability of the wave parameters is analyzed.

The interannual variability of storm waves recurrence with different thresholds (from 3 to 7 m) was calculated. A significant linear trend shows an increase in the storm wave frequency for the period from 1979 to 2017. A double growth in the reccurence was observed for cases with an SWH more than 3–5 m from 1979 to 2017. The local maximum of the storm waves more than 3–4 m was observed in 1995, and the minimum in 1998. The maximum value (four cases) of the number of storms with an SWH threshold 7 m is registered in 2016. The frequency of wind speeds and ice conditions contributing to the storm waves formation were analyzed. It is shown that trends in the storm activity of the Kara Sea are primarily regulated by the ice. If the ice cover decreases in the southern part of the sea that leads to the increase of the number of events only with SWH threshold more than 3–4 m. If in the entire sea the ice cover decreases that leads already to increase of the extreme storms. The frequency of strong and long-term winds has high interannual variability and a weak positive trend.

The analysis of distribution functions of the storm events with an SWH more than 3 m was carried out. Six different sectors of the Kara Sea were analyzed to reveal spatial differences. A comparison of the different distribution laws showed that the Pareto distribution is in the best agreement with the data. Up to 99% of the points are described by this distribution. However, the extreme events with an SWH more than 6–7 m deviate from the distribution, and their probability is approximately twice as less as that predicted by the Pareto distribution. Presumably, this deviation is caused by the combined impact of rare wind speed frequencies and anomalies of the sea ice conditions.

Keywords: Kara Sea, wave climate, storm activity, wind waves, wave modeling, WAVEWATCH III, probabilistic analysis, extreme waves

1. Introduction

The interest increases in the study of the hydrometeorological conditions of the Arctic seas due to the active economic development of this region. The active oil and mineral field exploration and development occur here, in this region. The Arctic is an area of intensive shipping and fishery. Wind, sea ice and wave conditions are limiting factors for the economic activity and the development of the infrastructure in the coastal zone. The storm waves can destruct the infrastructure facilities in coastal zones and offshore, a threaten human lifes and cause economic damage.

https://doi.org/10.5194/nhess-2020-198
Preprint. Discussion started: 7 July 2020

Natural Hazards and Earth System Sciences
Discussions

The construction of new facilities and the operation of existing ones need the risk and hazard assessment associated with impact of the storm waves. We need to study the extreme winds and waves in the past, their interannual variability because it possible to reduce the disasters risk in future.

Nowadays, storm activity is studied with several methods with use of different sources: direct observation data (De Leo et al., 2020; Menéndez et al., 2008), altimetry data (Meucci et al., 2020; Young and Ribal, 2019; Liu et al., 2016) and modeling data (Bertin et al., 2013; Dobrynin et al., 2015; Kurmar et al., 2016; Semedo et al., 2011; Wang and Swail., 2001; Weisse et al., 2005). There is also research work on wave heights in the 21st century Arctic Ocean (Khon et al., 2011). As direct measurements, especially in the Arctic Region, are very rare, and altimetry data are short series, thus the simulated data from models are preferable.

Regular and extreme characteristics of wind and waves of the Kara Sea are given in the Wind and Wave Climate Handbook of Russian Maritime Register of Shipping (2009). These data are based on the results of modeling. But the input wind forcing for the simulations was calculated from the atmospheric pressure data. Subsequently it was verified and calibrated by the weather stations measurements. Such information needs to be refined with the modern atmospheric reanalyses data. Diansky et al. (2014) describes some new results devoted to wave hindcast and forecast of the Kara Sea using the WRF wind.

Stopa et al. (2016) showed the main features of the wave climate and trends in the whole Arctic for the period 1992–2014. They noted that the ice cover decreases and at the same time the wave height rises. Liu et al. (2016) used satellite observations (1996–2015) for studying the wave climatology in the Arctic Ocean in summer (August–September). They show that winds and waves in the Barents and Kara Seas initially increased from 1996 to 2006 and later decreased until 2015.

Li et al. (2019) present details of the significant wave height (SWH) change with the retreat of the ice edge. The increase of the wave heights is shown for the Arctic subregions, including the Kara Sea.

Interannual variations of the mean and extreme SWH in ice-free conditions in the Kara Sea are described in (Duan et al., 2019). They estimated linear trends of SWH from 2005 to 2018, but these trends are not statistically significant for the most areas. The mean and extreme SWHs show relatively positive trends in the northeastern part of the Kara Sea, but the analysed period is too short for trend estimation (Duan et al., 2019).

Positive trends of the highest SWH and wind speed are shown for the Laptev and the Beaufort Seas based on the 38-year-long reanalysis. But for the Kara Sea trend analysis was not realised (Waseda et al., 2018).

The wind wave characteristics are studied in several researches for the whole world ocean (Young et al., 2011; Semedo et al., 2011; Kurmar et al., 2016). Semedo et al. (2011) described the seasonal variations of the global wave heights from 1957 to 2002 with the ERA-40 reanalysis data. In the Barents Sea the positive linear trend of SWH in winter months is observed Semedo et al. (2011). Zieger et al. (2013) calculated the mean and 99th SWH percentile for March and September in the Arctic based on the Envisat satellite data from 2002 to 2012.

However, in all mentioned studies there is no deep analysis of the storm interannual variability in the Kara Sea or the data series are too short to carry out it.

In (Kislov and Matveeva, 2020) studied the seasonal and interannual features of the Kara Sea meteorological regime and its connection with circulation indices. The period 2000-2010 is characterized by significant climate warming, a reduction of the surface of the old and first-year sea ice in the Arctic (Serreze et al., 2015; Caian et al., 2018; Shalina, 2013) and the appearance of a significantly larger ice-free sea surface than earlier. These highlights with the changing thermobaric structure of the atmosphere (Semenov et al., 2015; Semenov et al., 2018), and variability of Atlantic water inflow (Ivanov and Repina, 2018) can lead to the wind-wave regime changes in the Arctic Region. Such important features as modification of the cyclone number and its trajectories (Tilinina et al., 2014; Zhang et al., 2004), and the increase in daily extremes of wind speed (Surkova et al., 2015) were described. Also wind speeds rise to the north from 75–80° N in recent decades according to climatic reports (IPCC, 2013). Positive trends in average and extreme wind speeds in some parts of the Arctic Region are also noted in (Young and Ribal, 2019).

https://doi.org/10.5194/nhess-2020-198
Preprint. Discussion started: 7 July 2020

In this research, we present the wave reanalysis of the Kara Sea with a high spatial and temporal resolution. The regular and extreme wave characteristics were studied. The recurrence, trends and probability analysis of the storm waves in the Kara Sea were estimated for the long period from 1979 to 2017.

2. Data and Methods

2.1 Wave modeling

One of the main approaches of studying the world ocean wave climate is the spectral wave modeling that allows to create long-term reanalyses of wave parameters (Kurmar et al., 2016; Reistad et al., 2011; Semedo et al., 2011; Weisse et al., 2005;).

Modern spectral wave models provide high-quality results which are in good agreement with direct wave measurements. Correlation between model results and measurements data is usually 0.8–0.9, and the standard error is 0.3 m (Li et al., 2019, Reistad et al., 2011; Stopa et al., 2016).

The wave characteristics in the Kara Sea were calculated by the spectral wave model WAVEWATCHIII (WWIII) version 4.18 (Tolman, 2014). This model parameters considers wind speed, ice concentration, effects of the energy dissipation, non-linear interactions and bottom friction. This model is based on a numerical solution of the equation of the spectral wave energy balance:

$$\frac{\partial E(\omega, \theta, \vec{x}, t)}{\partial t} + \vec{V}(\omega, \theta)\nabla E = S(\omega, \theta, \vec{x}, t), \quad (1)$$

where ω and θ are the frequency and the propagation direction of the spectral component of the wave energy; $E(\omega, \theta, \vec{x}, t)$ is the two-dimensional spectrum of the wave energy at a point with vector coordinate $\vec{x}$ at time point t; $\vec{V}(\omega, \theta)$ is the group velocity of the spectral components; $S(\omega, \theta, \vec{x}, t)$ is a function that describes the wave energy sources and sinks, i.e., the transfer of the energy from the wind to the waves, nonlinear wave interactions, dissipation of the energy through collapse of the crests at a great depth and in the coastal zone, friction against the bottom and ice, wave scattering by ground relief forms, and reflection from the coastline and floating objects. The energy balance equation is integrated using finite-difference schemes by the geographic grid and the spectrum of wave parameters.

In present study, the calculations were made with the ST1 scheme (Tolman, 2014). A Discrete Interaction Approximation (DIA) model was used for the possible nonlinear interactions of the waves. The DIA is a standard approximation for the calculation of nonlinear interactions in all modern wave models.

Influence of the sea ice on the wave development was considered by the IC0 scheme, where a grid point is considered as ice-covered if ice concentration is >0.25. Thus, the exponential attenuation of wave energy adjusted for the sea ice concentration at a given point was added.

In the shallow water, the increase in wave height as waves approach the shore and the related wave breaking after waves reach the critical value of steepness were taken into consideration. The whitecapping effect taken into account in the ST1 scheme. The standard JONSWAP scheme was used to take the bottom friction into account. The spectral resolution of the model is 36 directions (Dq = 10°), the frequency range includes 36 intervals (from 0.03 to 0.843 Hz).

The calculations were performed using the unstructured grid, which consists of 16792 nodes (Fig. 1). The bathymetry data were obtained from the ETOPO 1-minute bottom topography database (https://www.ngdc.noaa.gov/mgg/global/) and detailed navigation maps. The grid covers the Barents and Kara seas, as well as the entire northern part of the Atlantic Ocean. The spatial resolution varies from ~15 km for the Kara Sea to ~50 km for the northern part of the Atlantic Ocean. The North Atlantic was included into the grid because of the swell propagating into the Barents and Kara seas, it was shown earlier in (Myslenkov et al., 2015).

https://doi.org/10.5194/nhess-2020-198
Preprint. Discussion started: 7 July 2020


Natural Hazards and Earth System Sciences Discussions

More detailed description of the model configuration, the main features of the experiments with the unstructured mesh is presented in (Myslenkov et al., 2018; Myslenkov et al., 2019). Wind and sea ice concentration data for the wave modeling were taken from the NCEP/CFSR reanalysis (1979–2010) with a spatial resolution ~ 0.3° (Saha et al., 2010) and NCEP/CFSv2 reanalysis (2011–2017) with a resolution ~ 0.2° (Saha et al., 2014), temporal resolution is 1 hour.

Figure 1

As a result, we got the wind wave fields for every three hours from 1979 to 2017 (total 39 years). The model results include the SWH (average value from 1/3 of the highest waves), the wave propagation direction, the mean wave period (WP) Tm02 and mean wave length (WL). Also, the wave heights of 1% and 3% probability of exceedance were used for the data analysis. These values were calculated as 1.51×SWH and 1.32×SWH, respectively (Coastal Egineering, 1995). The maximum and long-term SWH were calculated based on these data. When the Kara Sea was ice covered the wave parameters were equal to zero in model results. The mean long-term characteristics were performed for the ice-free period when the wave parameters were nonzero.

2.2 Recurrence of the storm waves

The storm activity analysis was held according to the Peak Over Threshold (POT) method, which is widely used (De Leo et al., 2020; Menéndez et al., 2008). This method was previously used for the Barents Sea (Myslenkov et al., 2019). The number of storm waves with different SWH from 3 to 7 m was calculated for each year in the Kara Sea or within the sea sector. The calculation procedure includes the following steps: if at least one node in the investigated sea area has the SWH exceeding a threshold, then such event is attributed to the storm case with waves more than this threshold. This event continues until the SWH will not be less than the threshold at all nodes of the investigated area. Further, if the threshold is exceeded in one of the nodes again, then this event is added to the following case. A period of 9 hours at least should pass between two storm cases for eliminating the possible errors. This technique has an inaccuracy associated with storms running in a row or from different directions at the same time. However, such cases are rare. The proposed algorithm works correctly, it was validated by a visual analysis conducted for several years.

The 3 m threshold was chosen as the 99% percentile of the entire studied period (1979–2017 in 3-hour interval) for the points in the central part of the sea (including the ice-covered periods) or as the 95% percentile for the ice-free period. There could be different criteria for the 95th percentile for regions of the Kara Sea. However, the aim of this research is deep analysis of the extreme events with the SWH exceeding 3 m for any points of the Kara Sea.

2.3 Quality assessment of the wave model results

Quality assessments of the modeling results based on the instrumental wave measurement data of the 1 mooring station in the Kara Sea (Fig. 2) for the period october 2012, published in [Atlas ..., 2015]. Wind wave measurements were carried out with upward-looking sonar IPS-5 for ice profiling. Data from this Atlas was digitized for statistical analysis.

Figure 2

A comparison of the modeled and measured SWH from September 1 to October 22, 2012 for mooring station is shown in Fig. 3. The model provides the absolute wave height and the phase of the individual storm event quite well. The result of the comparison for the entire data array is shown in Fig. 4. The correlation coefficient is 0.91, the BIAS is 0.08 m, and the RMSE is 0.31 m. The Scatter Index is 0.28. Further in the analysis the SWH values are presented with an accuracy of one decimal place during further analysis due to the obtained quality estimates.

Figure 3

Figure 4

The obtained quality assessments coincide with the assessments of other modern wave model implementations (Li et al., 2019, Reistad et al., 2011; Stopa et al., 2016). Good quality of the modeled data allows estimating the regular and extreme

https://doi.org/10.5194/nhess-2020-198
Preprint. Discussion started: 7 July 2020


Natural Hazards and Earth System Sciences
Discussions

characteristics of the wave climate, as well as the interannual variability of storm activity. We can conclude that WAVEWATCHIII with set configuration adequetly represents real conditions of the wind wave fields of the Kara Sea.

3. Results

3.1 Wave Climate

The general features of the wave climate in the Kara Sea are discussed in this chapter.

The distribution of the maximum SWH and mean long-term SWH for the Kara Sea for the modeling period (1979–2017) is shown in Fig. 5, a-d. The mean long-term SWHs are about 1.1–1.3 m (Fig. 5a) in the ice-free period. The maximum mean SWH is 1.3 m and observed in the northern part of the Kara sea. This area is associated with the influence of storms coming from the Barents Sea in the ice-free period. Formally the maximum SWH during the whole period reaches 9.9 m and is observed in the northern part of the sea, at the border with the Barents Sea (Fig. 5b). However, the wave conditions of this area are largely determined by the Barents Sea and this area belong to the Kara Sea because of the formal border. In the central part of the Kara Sea, the SWH maximum is 9.4 m and it is observed off the western coast of the Yamal Peninsula (Fig. 5b). The maximum wave height of a 3% probability is 12.4 m (Fig. 5, c), and a 1% probability is 14.3 m (Fig. 5, d) for the central part of the sea.

Figure 5

The Maritime Register Data (Wind and Wave ..., 2009) shows that the SWH with return period of 50 years is 5.4 m, and for a 1% probability of exceedance it is 7.8 m. Our results differ strongly from these estimates. It is explained by the model configurations and better wind forcing. Provided quality assessments for wave model results allow confessing the success of this particular implementation. The modeling period is also important because the ice conditions become milder since 2009, so the number of extreme storms increases (see next chapter).

A map of the long-term average probability of the ice occurrence is shown in Fig. 6, obtained from the NCEP/CFSR/CFSv2 reanalysis data. This map is used for the analysis of the distribution of the maximum SWH and long-term mean SWH. In general, the maximum values of SWH and mean SWH are concentrated in the ice-free areas.

Figure 6

According to long-term mean SWH fields and to maximum SWH values, at least we can reveal two large regions with particular spatio-temporal patterns of wave conditions, in the Kara Sea. The first one is the northern part which is often occupied by the ice. It is affected by storms from the Barents Sea in the ice-free periods. The second region is the southwestern part of the sea (Fig. 5-6). This region has longer ice-free period and wave generation occur without the influence of the Barents Sea. It should be pointed that in the north-eastern part of the Kara Sea the influence of storms from the Barents Sea should be expected, but, due to the high probability of the ice presence (> 0.8) in this region, the wave height is significantly lower than in other parts of the sea.

The next step of our research was seasonal analysis of the SWH maximum for four periods: December-January-February (DJF), March-April-May (MAM), June-July-August (JJA), September-October-November (SON). Figure 7 shows the SWH maximum for different periods of the year for the entire simulated period. Seasonal maximal SWH variability is also influenced by the ice conditions of the Kara Sea. Probability maps of the ice presence (with a concentration of more than 50%) for the same seasonal periods according to reanalysis are shown in Fig. 8.

Figure 7

Figure 8

For the March-May period, the SWH does not exceed 4.5 m (Fig. 7a) due to the ice presence for almost the entire period (Fig. 8a). The Kara Sea is free from ice in this period for a short time and in small areas. There is only one local SWH maximum (8.1 m) in the southern part of the sea in June-August (Fig. 7b). During this period, wind speed is usually less than

https://doi.org/10.5194/nhess-2020-198
Preprint. Discussion started: 7 July 2020


Natural Hazards and Earth System Sciences Discussions

in November-December therefore, severe storms are very rare despite the long ice-free period. Several SWH maxima are observed in September-November, including the 9.4 m height in the central part of the sea (Fig. 7c). This maximum is an absolute multi-year maximum for the central Kara Sea (Fig. 5b). Ice occurs only in the northern Kara Sea in this period (Fig. 8c). The strongest winds are observed in December -February. Most of the Kara Sea is ice-covered and the generation and propagation of wind waves are limited. However, severe storms from the Barents Sea pass to the northern Kara Sea during short ice-free periods. The absolute SWH maximum (9.9 m) for the entire sea was recorded was recorded there (Fig. 7a). The differences in the wave characteristics in Figures 7a and 7d are mainly associated with the features of the atmospheric circulation because the ice distribution is very similar in March-May and December-February (Figs. 8a and 8d).

The mean and maximum values of the average wave period and average wavelength are presented below. The long-term mean WP is 3.5 s (Fig. 9a). Such small WP is due to the long ice period and as consequence wave fetch is short. Mean WP corresponds to the mean long-term SWH of 1 – 1.3 m. The maximum WP is 8.4 s for the central Kara Sea and 10 s for the northern Kara Sea. The big WP is caused by several storms that come from the Barents Sea, where fetch is significantly greater and swell has a longer period. The average wavelength is 30 m for the central Kara and 35–40 m for the northern Kara (Fig. 9 c). The maximum wavelength is from 160 m and up to 300 m (Fig. 9 d) for the central and northern Kara respectively. However, large values are due to the calculating peculiarities of wavelength in spectral models. The remnant swell with an insignificant wave height can provide a peak period of up to 20 s and a long wavelength in almost calm conditions, but these values should not be considered as extreme.

Figure 9

3.2 Storm recurrence

The number of storm events per year was calculated in the Kara Sea according to the POT method (the technique is described in Chapter 2.2). The events have different SWH thresholds from 3 to 7 m. Next, we will call these storm events with a different wave height simply a storm. At first, we analyzed the number of storms for each year (Fig. 10), which called recurrence of storm. Cases of storms with the SWH ≥ 3 m were observed about 30 times per year. Number of storms with the SWH ≥ 4 m is about 15 times. The most severe storms with a threshold 7 m were not registered each year. The maximum number of storms with SWH ≥ 3 m was in 2016. It is noteworthy, that in 2016 peaks were also registered for all other thresholds and the recurrence of the most severe events ≥ 7 m is the highest. A local maximum number of storms with SWH thresholds 3 and 4 m was noted in 1995. The minimum numbers of storms for several SWH thresholds were noted in 1998 and 2003. A linear positive trend in the number of storms is observed for almost all SWH thresholds. A double increase of storm recurrence was observed for cases with thresholds 3–5 m from 1979 to 2017. It's worth noting that there is high interannual variability in the number of storms. The average variance is about 25–30 % from year to year.

The significance of trends was assessed by the F-test. Trends for the number of weaker storms more than 3–4 m are significant at the level p = 0.05. For more severe storms with SWH thresholds 5–7 m, trends are statistically insignificant. Similar result were obtained for 2005 to 2018 (Duan et al., 2019).

Figure 11

The analysis of the ice concentration variability in the Kara Sea was performed to explain the interannual variability of the storminess. The graphs of ice probability for two points in the Kara Sea is presented in Figure 11. Ice probability is the ratio of number of days with observed ice to the duration of the whole year. The points were selected in the central and southern parts of the Kara Sea to demonstrate the difference of the ice conditions. There is a significant negative trend in the variability of ice cover. Ice probability is approximately twice as less from 1979 to 2017. This trend is observed at both points. It can be assumed that ice cover decreases in the whole sea. This fact has been detected by various researchers previously (Cavalieri and Parkinson, 2012; Caian et al., 2018; Comiso et al., 2017; Maslanik et al., 2011; Serreze and Stroeve, 2015). The ice probability decreases from 0.7 to 0.55 in center of Kara Sea (T1 point). The decrease is even greater in the southern Kara

https://doi.org/10.5194/nhess-2020-198
Preprint. Discussion started: 7 July 2020


Natural Hazards and Earth System Sciences Discussions

(T2): from 0.7 to 0.4 (Fig. 11). A local minimum of the ice probability was noted in 1995 in the southern part of the Kara Sea. This minimum probably led to an increase of the number of storms with SWH ≥ 3 and 4 m (Fig. 10). But in 1995 ice cover reduction was observed only in the southern Kara, not in the whole sea, that's why such reduction does not cause extreme storms (≥5 m). The maximum ice cover was observed in 1998–1999 and amounted to 0.8 in both points. It led to the storminess weakening (Fig. 10). The ice probability minima were observed in 2012 and 2016 in T1 and T2. These minima coincide with a significant increase in number of storms (including storms with SWH ≥7 m) that was observed exactly in these years.

Figure 11

Also, we analyzed the interannual variability of the wind conditions in the Kara Sea to explain the interannual variability of storm recurrence. The relationship between wind speed and wave height is non-linear. In addition, we need to consider such factors as fetch length, ice presence, and duration of wind impact. Therefore, correlation analysis for the wind recurrence with defined speed (higher than threshold values) and wind duration time with the storm repeatability was performed. The average daily wind speed at 10 m above the sea level was obtained from the reanalyses NCEP/CFSR and NCEP/CFSv2 for the period 1979–2017 for two points (the same as for the ice probability analysis points): T1, 66.04 °E, 73.91 °N; and T2, 61.59 °E, 71.09 °N. The maximum correlation (0.65) is observed in a comparison of the number of storms with SWH threshold 4 m and wind recurrence with speeds greater than 10 m/s, it was revealed for 2 continous days at T1. These storm wind conditions were used as an indicator in the analysis of the interannual variability of the wind.

The recurrence of storm wind conditions, number of storms with SWH more than 4 m, and the ice probability are shown in Fig. 12. The recurrence of storm wind conditions agrees quite well with the recurrence of storms. It is also seen that years with high sea ice conditions reduce the number of storms in 1998 and 2003 despite the average values of storm wind conditions. The significance of trends was estimated by F-test. Trends of the storm waves recurrence and the ice probability are significant at the level of 0.05, and the trend of the storm wind recurrence is statistically insignificant.

Figure 12

Thus, there is a evident positive trend for number of storms in the Kara Sea according to the results of the analysis. This trend is mainly caused by the sea ice cover decrease over the past 40 years, the trend of storm wind conditions is not statistically significant. The interannual variability of events with SWH more than 3–4 m correlates quite well with the wind recurrence (speeds more than 10 m/s). However, both wind and ice conditions, certainly affect the storminess. Ice cover reduction leads to an increasing of weaker storms SWH ≥ 3–4 m in the southern Kara Sea. Such reduction in the entire sea leads to the increase of extreme storms number (SWH > 5–7 m). The influence of ice cover variability also were obtained in the work (Li et al., 2019).

Climate changes in storm wind conditions may be associated with changes in the ice conditions in the Kara Sea, however, this analysis is already beyond the scope of our research and requires more detailed study. It is a challenge task for future research.

3.3 Probability analysis of storm waves in different sectors of the Kara Sea.

Based on the analysis of the mean long-term and seasonal variability of the wave heights, the Kara Sea was divided into several sectors with different wave conditions. In these areas, several zones of maximum waves are observed in different periods of the year (Fig. 7a–d). This segmentation allows to analyze extreme storms in detail.

Figure 13

A catalog of storms with SWH more than 3 m was formed for each sector shown in Fig. 10. The POT method was used to create the catalog, and a threshold of 3 m was chosen as the 95th percentile for the sample for the ice-free period. In this catalog, each member of the series is a separate storm event. It is necessary condition for the independence of the members of the series according to the method of "independent storms" (Cook, 1982). The length of the data series is sufficient for statistical analysis. Series consists of 450–750 values depending on the sector.

https://doi.org/10.5194/nhess-2020-198
Preprint. Discussion started: 7 July 2020

Natural Hazards and Earth System Sciences
Discussions

The storm data series for each of the 6 sectors were approximated by various distribution functions. A comparison of the functions with the empirical data showed that the best approximations for the storm recurrence was the Pareto distribution

$$F(H) = 1 - \left(\frac{H_{th}}{H}\right)^{\gamma}, \quad (2)$$

where H_{th} is the threshold value. γ is the distribution parameter easily determined by the least square. For this purpose, formula (2) by logarithm is reducing to

$$ln\big(1 - F(H)\big) = -\gamma \cdot \ln(H) + \gamma \cdot \ln(H_{th})\,. \quad (3)$$

If the empirical values on the diagram are located along a straight line in the logarithmic coordinates, this means that the empirical distribution corresponds to the Pareto distribution. The quantitative correspondence of the empirical and the theoretical distribution is established by using known statistical criteria.

Pareto distribution for all sectors is shown in Fig. 14. About 99% of the points are described by the Pareto distribution with parameters H_{th} = 3 m and γ = 4.8 and a determination coefficient of R^2 = 0.98 in sector 6. This approximation is used as base distribution. The Kolmogorov-Smirnov test also shows that the Pareto distribution is quite well. A similar pattern of distribution functions is observed for all six sectors.

Figure 14

The average value of γ is equal to 4.6 (varying from 4.2 to 5.0 for different sectors). The proximity of the parameters in the Pareto distribution indicates that the extrema are generated in all sectors with a similar law. Thus, the wave generation with an SWH more than 3 m is determined by the same mechanism. The basis of the hypothesis is the series of extrema determined by the same law of probability distribution. A similar analysis is given in (Taleb, 2010). All extreme events are called “swans”, while the maximum and the largest rare events are “black swans”. However, there are very rare cases when the empirical distribution deviates and exceeds the base distribution in the large values area. These unique events are called “dragons” (Sornette, 2009). The extreme values of SWH greater than 8 m observed in 2, 4, 5 sectors.

In our case, several extreme values that deviate from the base distribution were detected in each sector due to the analysis of the distribution functions. The direction is common to these deviations - the points always deviate upward (Fig. 14). Therefore, these events are “dragons”. A similar principle was used for freak wave detection (Buhler, 2007) and in studying wind speed extremes (Kislov and Matveeva, 2016; Kislov and Platonov, 2019; Platonov and Kislov, 2019). Unique extrema “dragons” falling out of the base distribution and have a different distribution law and, probably, a different genesis.

It is very important that the probability of extreme events based on a theoretical function, in our case, the Pareto distribution. For example, the data of sector 6 (East coast of Novaya Zemlya) (Fig. 14) shows an SWH equal to 6.7 m (logarithm 1.9) – almost the last value that still lies on the base Pareto distribution. This value repeated through 47 sample elements ($\left(\frac{H}{H_{th}}\right)^{\gamma}$) on average. However, storms with such SWH occurs about a 100 times in reality (Fig. 14), twice as much as it was planned by the Pareto approximation. A similar situation is reflected for the other sectors in the “dragons” zone. Use of base distribution in this zone leads to incorrect probability calculation results. This fundamental result demonstrates the source of systematic errors in evaluating the recurrence of extreme wave heights, which are especially relevant in applied and forecast tasks.

The probability of “dragons” doesn’t match the base distribution. In the Kara Sea, the occurrence of storms with high waves depends on several factors simultaneously: primarily on the wind speed, direction, and duration of the wind, secondly on the ice conditions (fetch limit) or the influence of the Barents Sea (for 4-th sector). The number of storms with SWH more than 3–4 m is closely related to wind speed and wind duration as it was shown in chapter 3.2, but the repeatability of storms with SWH more than 6–8 m requires the simultaneous combination of small ice cover and extreme wind conditions. Thus, the division of the empirical distribution function between “black swans” and “dragons” occurs when the influence of small ice cover (and consequently more long fetch) is observed besides the wind forcing. Since wind and ice conditions are considered as approximately independent events, their joint probability is much lower than the probability of rare wind events.

https://doi.org/10.5194/nhess-2020-198
Preprint. Discussion started: 7 July 2020


Natural Hazards and Earth System Sciences Discussions

Extreme events with any (even very large) wave height can occur according to the base distribution function, formally. However, the empirical function for the "dragons" is nonlinear and goes to a certain plateau; it was shown in the logarithmic graphs. The γ values (starting with some values of H) begin to increase rapidly. Thus, there is a certain natural limit observed for extreme events. "Dragons" have a limitation for maxima wave height that differs from the base distribution. The basic distribution ends in the range of SWH values 6.5–8 m in different sectors. Such differences are associated with the definition of freak waves in the article (Buhler, 2007). Freak waves are unique anomalous individual waves that do not correspond to the general distribution. In our case, we have a similar picture on the synoptic scale, where specific storms with a certain SWH maximum defined as "dragons".

Figure 15 shows the graph of "dragons" passing by year in each of the six sectors. This graph was analyzed for the possible impact of climate change on the "dragon" recurrence. "Dragons" occurred in sectors 1 and 5 only after 1997-2000, when the increased recurrence was registered for the entire Kara Sea. A higher recurrence of "dragons" was registered in years when there were simultaneous peaks of wind recurrence and small sea ice cover (see Fig. 13).

Figure 15

Thus, a reduction of the sea ice cover and increased recurrence of stronger winds lead to an increase of the extreme wave heights. There are climatic changes in the "dragon" repeatability, that increased due to the ice cover reduction in the last 40 years.

Discussions and Conclusions

A wave climate and storm recurrence in the Kara Sea has been presented based on the results of wave modeling. The SWH, the mean WP, and mean WL fields were obtained for every three hours from 1979 to 2017 (39 years in total). The mean SWH for the entire sea varies from 1.1 to 1.3 m. The SWH maximum is 9.9 m and it is observed in the northern part of the Kara Sea. Analysis of maxima for different times of year showed that the SWH does not exceed 4.5 m in March-May. The wave generation is limited by the ice presence in some periods of the year. The long-term mean wave period value is 3.5 sec and the average wave lenght is 30 m for the central Kara and 35–40 m for the northern part.

The storm recurrence with an SWH threshold from 3 to 7 m was calculated in the Kara Sea for each year according to the POT method. Storms with an SWH ≥3 m are observed about 30 times per year on average, with SWH more than 4 m - about 15 times. Storms with a threshold of 7 m are not observed every year. The storminess was higher in 1994–1995 and after 2008. The minimum numbers of storms were registered in 1998 and 2003.

The combined analysis of the storm activity, the recurrence of strong winds, and the ice probability was carried out. The high recurrence of strong winds and the absence of sea ice lead to increase of storm number with SWH 3–4 m in the southern Kara Sea. When the sea ice probability decreases for the whole sea and recurrence of strong winds is high simultaneously, then the number of extreme storms (SWH more than 5–7 m) increases.

There is an obvious positive trend of the storm activity in the Kara Sea and a positive linear trend of the weaker storm recurrence (SWH more than 3–4 m) for 1979 – 2017. Linear trend of the severe storm recurrence (SWH more than 5–7 m) is positive but statistically insignificant because such events are rare. This trend is mainly caused by a reduced sea ice cover over the past 40 years, the trend in recurrence of storm wind conditions is not significant.

The Kara Sea was divided for six sectors with different wave conditions due to the analysis of the mean long-term and seasonal variability of wave heights.

The probability analysis for the six sectors of the Kara Sea was provided. Different approximations were compared with the empirical distribution, the best approximation for the storm recurrence was the Pareto distribution. The proximity of the parameters in the Pareto distribution indicates that the extrema generation occurs in the same way for all sectors.

https://doi.org/10.5194/nhess-2020-198
Preprint. Discussion started: 7 July 2020


Natural Hazards and Earth System Sciences Discussions

Analysis of the distribution functions for each of the sectors showed that several extreme events ("dragons") deviate upward from the base Pareto distribution. Thus, the division of the empirical distribution function between "black swans" and "dragons" occurs when the influence of small ice cover (and consequently more long fetch) is observed besides the wind forcing. "Dragons" occurred in sectors 1 and 5 only after 2000, when the increased recurrence was registered for the entire Kara Sea. A higher recurrence of "dragons" was registered in years when there were simultaneous peaks of wind recurrence and small sea ice cover. On a time scale of 40 years, we see climatic changes in increasing the recurrence of such extreme events as "dragons".

There are some questions of the quality assessment of the wave model for extremely high waves, but unfortunately, we do not have full-scale direct measurement data in the Kara Sea, and satellite data also need verification and are not accurate.

In this paper, we do not consider the relationship between number of storms variability with global climatic indices of large scale atmposphere circulation. Earlier in (Myslenkov et al., 2019), we showed that for the Barents Sea the number of storms only of extreme events with SWH ≥ 7 m and only for the DJF has a low correlation with the Arctic Oscillations index. And this is largely due to the decisive influence of the Atlantic on the Barents Sea. In the Kara Sea, the influence of the Atlantic and Western transport is even less, therefore, probably there is no connection with global indices here. On the other hand, we showed that the wave climate in the Kara Sea is regulated by ice cover variability. Connection between sea ice loss and the Arctic Oscillation detected in (Yang et al., 2016), therefore theoretically it is possible to find a connection between wave climate of the Kara Sea and global indexes, what are we going to do in the future.

Data availability

Data and results in this article resulting from numerical simulations are available upon request from the corresponding author.

Author contributions

The concept of the study was jointly developed by SM. SM did the numerical simulations, analysis, visualization and manuscript writing. VP and AK did the probability analysis of storm waves and its visualization. KS analysed the results of numerical modeling. IM did the validation of the model. SM prepared the paper with contributions from VP, AK, KS and IM.

Competing interests.

The authors declare that they have no conflict of interest.

Acknowledgments.

The wave modeling and probabilistic analysis were done with the financial support of the RFBR (project 18-05-60147 Myslenkov S.A., Platonov V.S., Kislov A.V.).

Data analysis funded by the Ministry of Science and Higher Education of Russia, theme 0149-2019-0004, and RFBR project 20-35-70039 (Silvestrova K.P).

Validation of the model done by I.P. Medvedev with the financial support of the RFBR (project 18-05-60250).

Authors gratefully thank A.Yu. Medvedeva for the editorial remarks.

References

Atlas of hydrometeorological and ice conditions of the seas of the Russian Arctic «Oil Industry », 2015. – 128 p

Bertin X, Prouteau E, Letetrel C (2013) A signifcant increase in wave height in the North Atlantic Ocean over the 20th century. Global Planet Change 106:77–83

https://doi.org/10.5194/nhess-2020-198
Preprint. Discussion started: 7 July 2020

Natural Hazards and Earth System Sciences
Discussions

Buhler O (2007) Large deviation theory and extreme waves. Proc. Aha Huliko'a Hawaiian Winter Workshop University of Hawaii at Manoa, January 23–26, 2007 pp. 9-18.

Caian M, Koenigk T, Döscher R. et al. (2018) An interannual link between Arctic sea-ice cover and the North Atlantic Oscillation. Clim Dyn 50, 423–441. https://doi.org/10.1007/s00382-017-3618-9

Cavalieri D, and Parkinson C (2012) Arctic sea ice variability and trends, 1979–2010. Cryosphere, 6, 881–889, https://doi.org/10.5194/tc-6-881-2012.

Coastal Engineering – Waves, Beaches, Wave-Structure Interactions. Edited by T. Sawaragi Volume 78, Pages 1-479 (1995).

Comiso J, Meier W and Gersten R (2017) Variability and trends in the Arctic Sea ice cover: Results from different techniques. J. Geophys. Res. Oceans, 122, 6883–6900, https://doi.org/10.1002/2017JC012768.

Cook N (1982) Towards better estimation of wind speeds. J. Wind Eng. Ind. Aerodyn. 9. 295–323.

De Leo F, Solari S Besio G (2020) Extreme wave analysis based on atmospheric pattern classification: an application along the Italian coast. Nat. Hazards Earth Syst. Sci., 20, 1233–1246, https://doi.org/10.5194/nhess-20-1233-2020.

Diansky N, Fomin V, Kabatchenko I, Gruzinov V (2014) Simulation of circulation of the Kara and Pechora Seas through the system of express diagnosis and prognosis of marine dynamics. Arctic: ecology and economy. 1(13). 57-73.

Dobrynin M, Murawski J, Baehr J and Ilyina T (2015) Detection and attribution of climate change signal in ocean wind waves. J. Climate, 28, 1578–1591, https://doi.org/10.1175/JCLI-D-13- 00664.1.

Duan C, Dong S, Wang Z (2019) Wave climate analysis in the ice-free waters of Kara Sea Reg. Stud. Mar. Sci. Article 100719

IPCC (2013) Summary for Policymakers. In: Climate Change 2013: The Physical Science Basis. Contribution of Working Group I to the Fifth Assessment Report of the Intergovernmental Panel on Climate Change / Eds T.F. Stocker, D. Qin, G.-K. Plattner et al. Cambridge, United Kingdom and New York, NY, USA, Cambridge University Press.

Ivanov V and Repina I (2018) The Effect of Seasonal Variability of Atlantic Water on the Arctic Sea Ice Cover. Izv. Atmos. Ocean. Phys. 54, 65–72.

Kislov A and Matveeva T (2016) An extreme value analysis of wind speed over the european and siberian parts of arctic region. Atmospheric and Climate Sciences. 6. 205–223.

Kislov A and Matveeva T (2020) The Monsoon over the Barents Sea and Kara Sea. Atmospheric and Climate Sciences. 10. 339-356.

Kislov A and Platonov V (2019) Analysis of observed and modelled near-surface wind extremes over the sub-arctic northeast Pacific. Atmospheric and Climate Sciences, 9(1):146–158, 2019. http://dx.doi.org/10.4236/acs.2019.91010

Khon V, Mokhov I, Pogarskiy F, Babanin A, Dethloff K, Rinke A and Matthes H (2014) Wave heights in the 21st century Arctic Ocean simulated with a regional climate model. Geophys. Res. Lett. 41, 2956–2961.

Kumar P, Min S.-K., Weller E, Lee H and Wang X (2016) Influence of climate variability on extreme ocean surface wave heights assessed from ERA-Interim and ERA-20C. J. Climate, 29, 4031–4046, https://doi.org/10.1175/JCLI-D-15-0580.1

Li Jingkai, Ma Y, Liu Q, ZhangW and Guan C (2019) Growth of wave height with retreating ice cover in the Arctic. Cold Regions Science and Technology, 164, 102790. doi: 10.1016/j.coldregions.2019.102790

Liu Q, Babanin A, Zieger S, Young I and Guan C (2016) Wind and wave climate in the Arctic Ocean as observed by altimeters. J. Climate. 29(22). 7957–7975.

Lopatoukhin L, Rozhkov V, Ryabinin V, Swail V, Boukhanovsky A and Degtyarev A (2000) Estimation of extreme wind wave heights. WMO/TD-No. 1041, JCOMM Technical Report No. 9.

Maslanik J, Stroeve J, Fowler C and Emery W (2011) Distribution and trends in Arctic sea ice age through spring 2011. Geophys. Res. Lett., 38, L13502, doi: https://doi.org/10.1029/2011GL047735.

https://doi.org/10.5194/nhess-2020-198
Preprint. Discussion started: 7 July 2020

Menéndez M, Méndez F, Losada I and Graham N (2008) Variability of extreme wave heights in the northeast Pacific Ocean based on buoy measurements, Geophys. Res. Lett., 35, L22607, doi:10.1029/2008GL035394.

Meucci A, Young I, Aarnes O and Breivik Ø (2020) Comparison of Wind Speed and Wave Height Trends from Twentieth-Century Models and Satellite Altimeters. J. Climate, 33, 611–624

Myslenkov S, Markina M, Arkhipkin V, Tilinina N (2019) Frequency of storms in the Barents sea under modern climate conditions. Vestnik Moskovskogo Universiteta, Seriya 5: Geografiya. 2. 45-54.

Myslenkov S, Markina M, Kiseleva S et al. (2018) Estimation of Available Wave Energy in the Barents Sea. Thermal Engineering. 65, 7, 411–419.

Myslenkov S, Medvedeva A, Arkhipkin V, Markina M, Surkova G, Krylov A, Dobrolyubov S, Zilitinkevich S, and Koltermann P (2018) Long-term statistics of storms in the Baltic, Barents and White Seas and their future climate projections. Geography, Environment, Sustainability. 11. 1. 93–112.

Myslenkov S, Arkhipkin V, Koltermann K (2015) Evaluation of swell height in the Barents and White Seas. Moscow University Bulletin, Series 5. Geography. 5. 59-66.

Platonov V and Kislov A (2019) Spatial distribution of extreme wind speeds statistics over the Sakhalin island based on observations and high-resolution modelling data. IOP Conference Series: Earth and Environmental Science, 386(012). http://dx.doi.org/10.1088/1755-1315/386/1/012052

Reistad M, Breivik Ø, Haakenstad H, Aarnes OJ, Furevik BR (2011) A high-resolution hindcast of wind and waves for the North Sea, the Norwegian Sea and the Barents Sea. J Geophys Res 116, C05019

Saha S. et al. (2010) The NCEP climate forecast system reanalysis. Bul. of the American Meteorological Society. 91. 8. 1015–1057.

Saha S. et al. (2014) The NCEP Climate Forecast System Version 2. J. Climate. 27, 2185—2208

Semedo A, Sušelj K, Rutgersson A, Sterl A (2011) A global view on the wind sea and swell climate and variability from ERA-40. J Clim 24(5):1461–1479

Semenov E, Sokolikhina N, Tudriy K and Shchenin M (2015) Synoptic Mechanisms of Winter Warming in the Arctic. Russian Meteorology and Hydrology. 40, 576-583. https://doi.org/10.3103/S1068373915090022

Semenov V and Cherenkova E (2018) Evaluation of the Atlantic Multidecadal Oscillation Impact on Large-Scale Atmospheric Circulation in the Atlantic Region in Summer. Dokl. Earth Sc. 478, 263–267

Serreze M and Stroeve J (2015) Arctic sea ice trends, variability and implications for seasonal ice forecasting. Philos. Trans. Roy. Soc. London, 373A, 20140159, doi:https://doi.org/10.1098/rsta.2014.0159

Shalina E (2013) Arctic sea ice decline from satellite passive microwave observations. Sovremennye problemy distantsionnogo zondirovaniya Zemli iz kosmosa. 10. 1. 328–336

Sornette D. (2009) Dragon-Kings, Black Swans and the Prediction of Crises. International Journal of Terraspace Science and Engineering. 2. 1–18

Stopa J, Ardhuin F,Girard-Ardhuin F (2016). Wave climate in the Arctic 1992-2014: seasonality and trends. Cryosphere, 10(4), pp.1605-1629.

Surkova G, Sokolova L, Chichev A (2015) Long-term regime of extreme winds in the Barents and Kara seas. Vestnik Moskovskogo universiteta. Serija 5: Geografija. 5. 53–58.

Taleb N (2010) The black swan: The impact of the highly improbable fragility. (New York, Random House). 300.

Tilinina N, Gulev S, Bromwich D. (2014) New view of Arctic cyclone activity from the Arctic System reanalysis. Geophys. Res. Lett. 43. 1766–1772

Tolman H (2014) The WAVEWATCH III Development Group User Manual and System Documentation of WAVEWATCH III version 4.18. Tech. Note 316, NOAA/NWS/NCEP/MMAB, available at: http://polar.ncep.noaa.gov/waves/wavewatch/ manual.v4.18.pdf (last access: 23 June 2018).

https://doi.org/10.5194/nhess-2020-198
Preprint. Discussion started: 7 July 2020

Natural Hazards and Earth System Sciences
Discussions

Wang X and Swail V (2001) Changes of extreme wave heights in Northern Hemisphere oceans and related atmospheric circulation regimes. J Clim 14:2204–2221

Waseda T, Webb A, Sato K, Inoue J, Kohout A, Penrose B (2018) Correlated increase of high ocean waves and winds in the ice-free waters of the Arctic Ocean. Sci. Rep. 8 (1). https://doi.org/10.1038/s41598-018-22500-9

Weisse R, Von Storch H, Feser F (2005) Northeast Atlantic and North Sea storminess as simulated by a regional climate model during 1958– 2001 and comparison with observations. J Clim 18:465–479

Wind and Wave Climate Handbook. Kara Sea and Sea of Japan (2009) Ed. by L. I. Lopatukhin, et al. (Russian Maritime. Register Shipping., St. Petersburg, 2009)

Young I and Ribal A (2019) Multiplatform evaluation of global trends in wind speed and wave height. Science. 364. 548–552. https:// doi.org/10.1126/science.aav9527

Young I, Zieger S and Babanin A (2011) Global trends in wind speed and wave height. Science. 332. 451–455. https://doi.org/ 10.1126/science.1197219

Yang X, Yuan X and Ting M (2016) Dynamical link between the Barents-Kara sea ice and the arctic oscillation. J. Climate. 29. 5103–5122

Zhang X, Walsh J, Zhang J, Bhatt U and Ikeda M (2004) Climatology and interannual variability of Arctic cyclone activity: 1948–2002. J. Climate, 17, 2300–2317, https://doi.org/10.1175/1520-0442(2004)017<2300:CAIVOA>2.0.CO;2

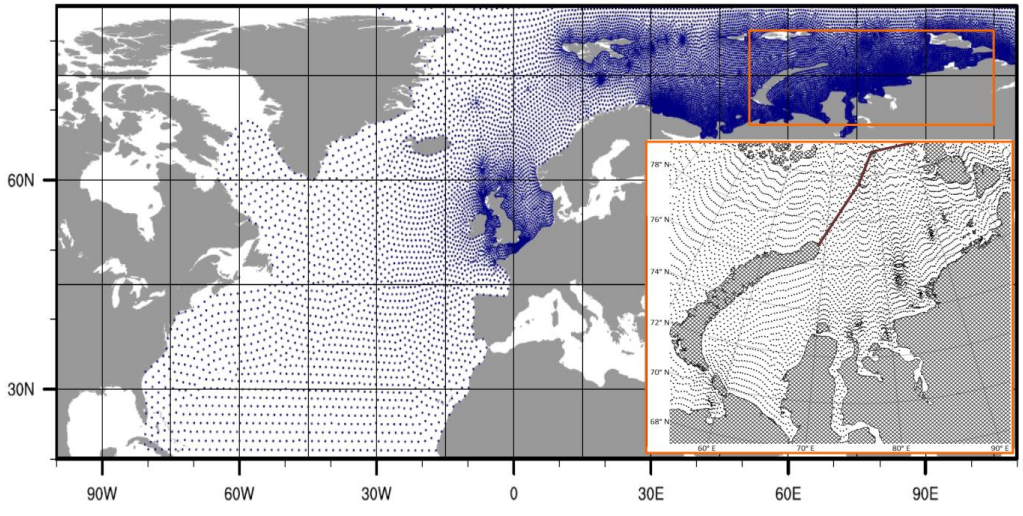

Figure 1. Unstructured computational grid for the North Atlantic and the Kara Sea.

https://doi.org/10.5194/nhess-2020-198
Preprint. Discussion started: 7 July 2020

Natural Hazards and Earth System Sciences
Discussions

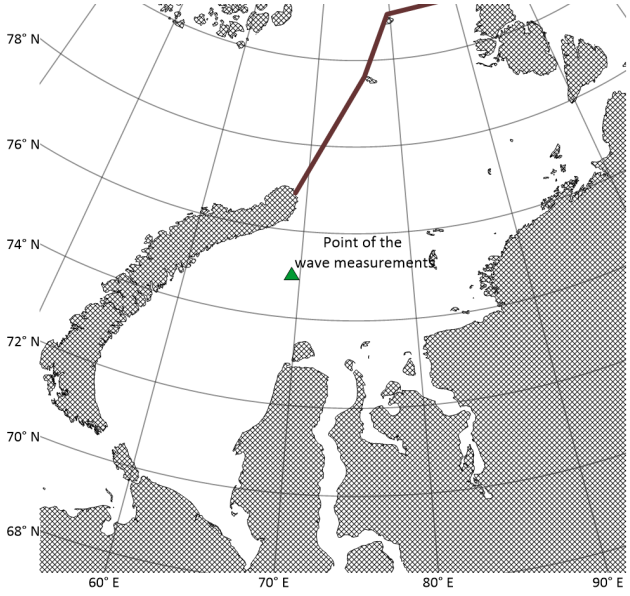

528

529 Figure 2. Location of the wave measurement stations (a), a histogram of the distribution of wave heights at station No. 3 (b).

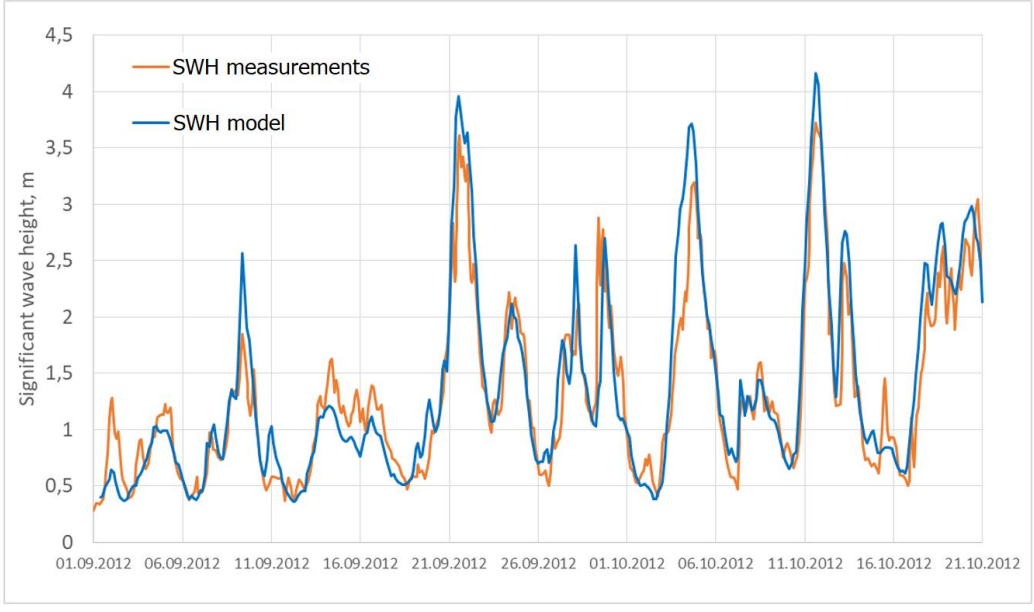

530

531 Figure 3. The measured and simulated SWH for station No. 5.

532

https://doi.org/10.5194/nhess-2020-198
Preprint. Discussion started: 7 July 2020

Natural Hazards and Earth System Sciences
Discussions

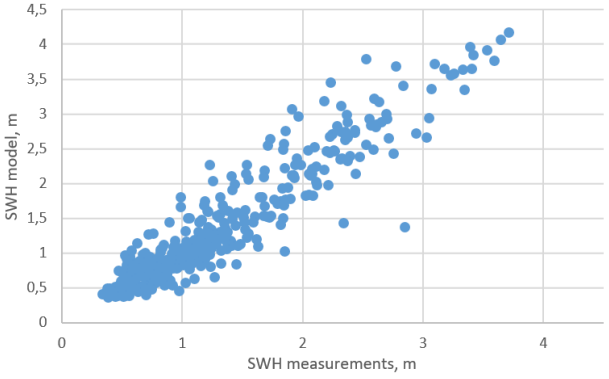

Figure 4. Scatter diagram of measured and simulated SWH for all points

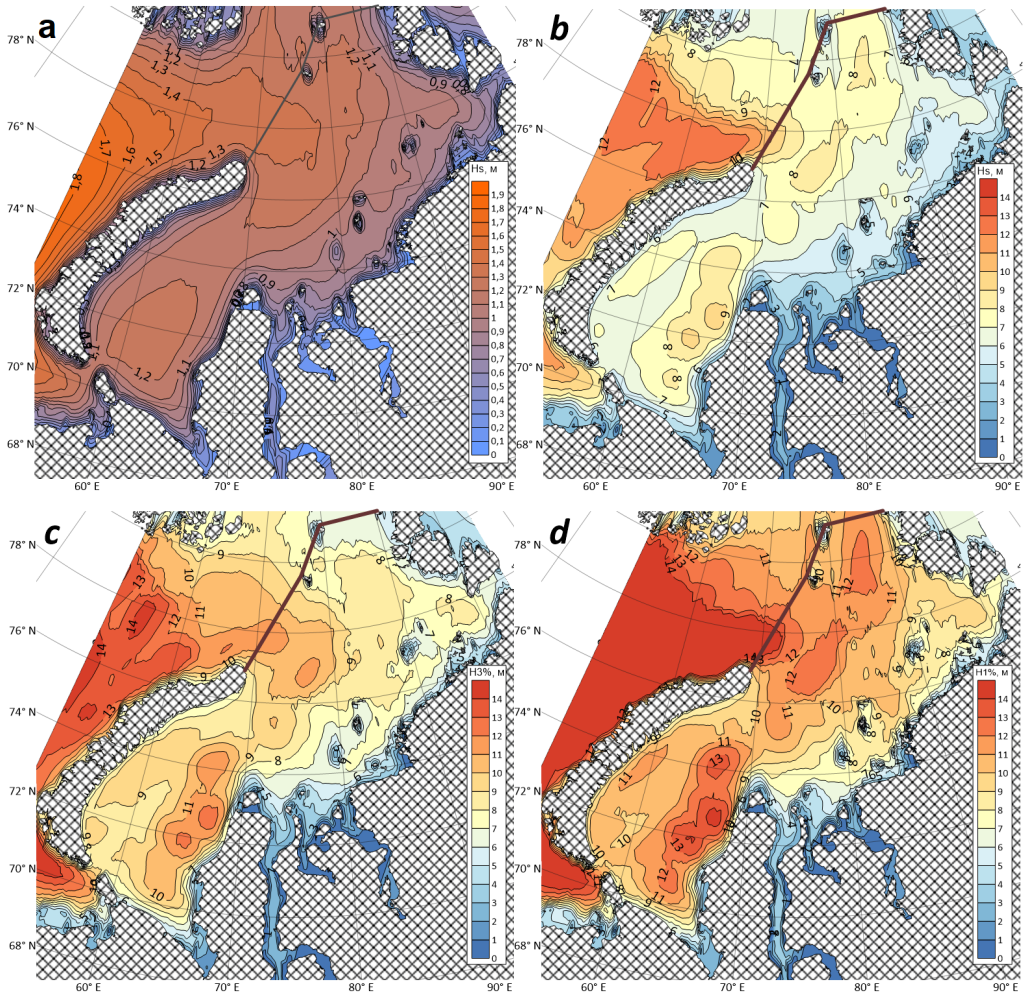

Figure 5. The long-term mean (a), maximum (b) significant wave heights, maximum wave height of 3% probability of exceedance (c), and maximum wave height of 1% probability of exceedance (d) according to the modeled data in the Kara Sea for the 1979–2017 period.

https://doi.org/10.5194/nhess-2020-198
Preprint. Discussion started: 7 July 2020

Natural Hazards and Earth System Sciences
Discussions
Open Access
EGU

542

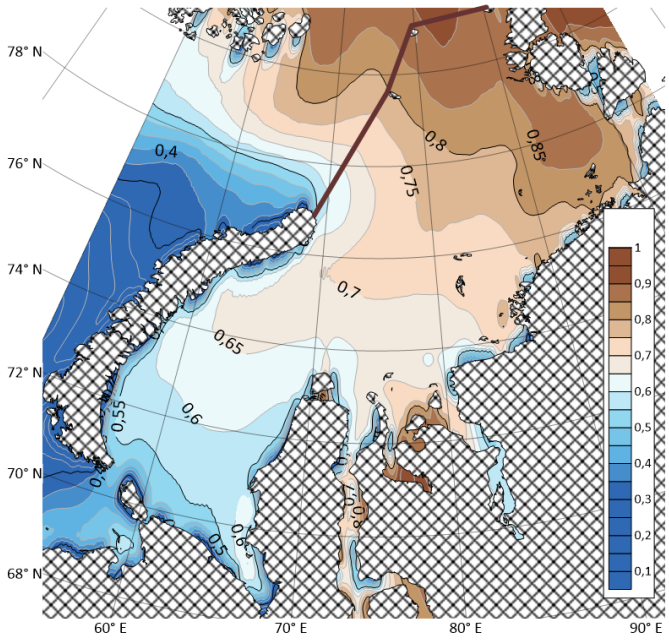

543

544 Figure 6. The long-term average probability of the ice presence of with a concentration more than 50% in the Kara Sea
545 according to reanalysis data from 1979 to 2017 (in 0–1 unit).

546

https://doi.org/10.5194/nhess-2020-198
Preprint. Discussion started: 7 July 2020

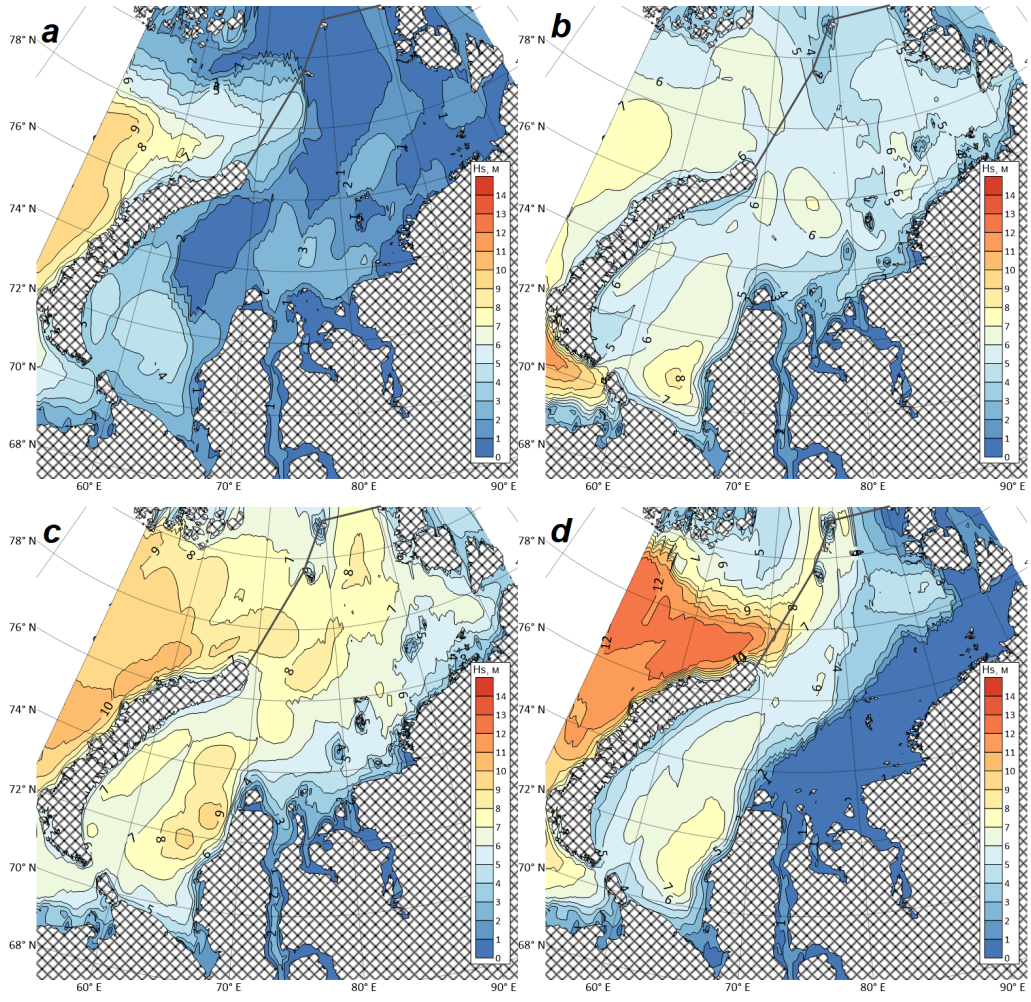

Figure 7. The maximum SWH in the Kara Sea according to the model data (from 1979 to 2017) for the periods: MAM (a), JJA (b), SON (c), DJF (d).

https://doi.org/10.5194/nhess-2020-198
Preprint. Discussion started: 7 July 2020

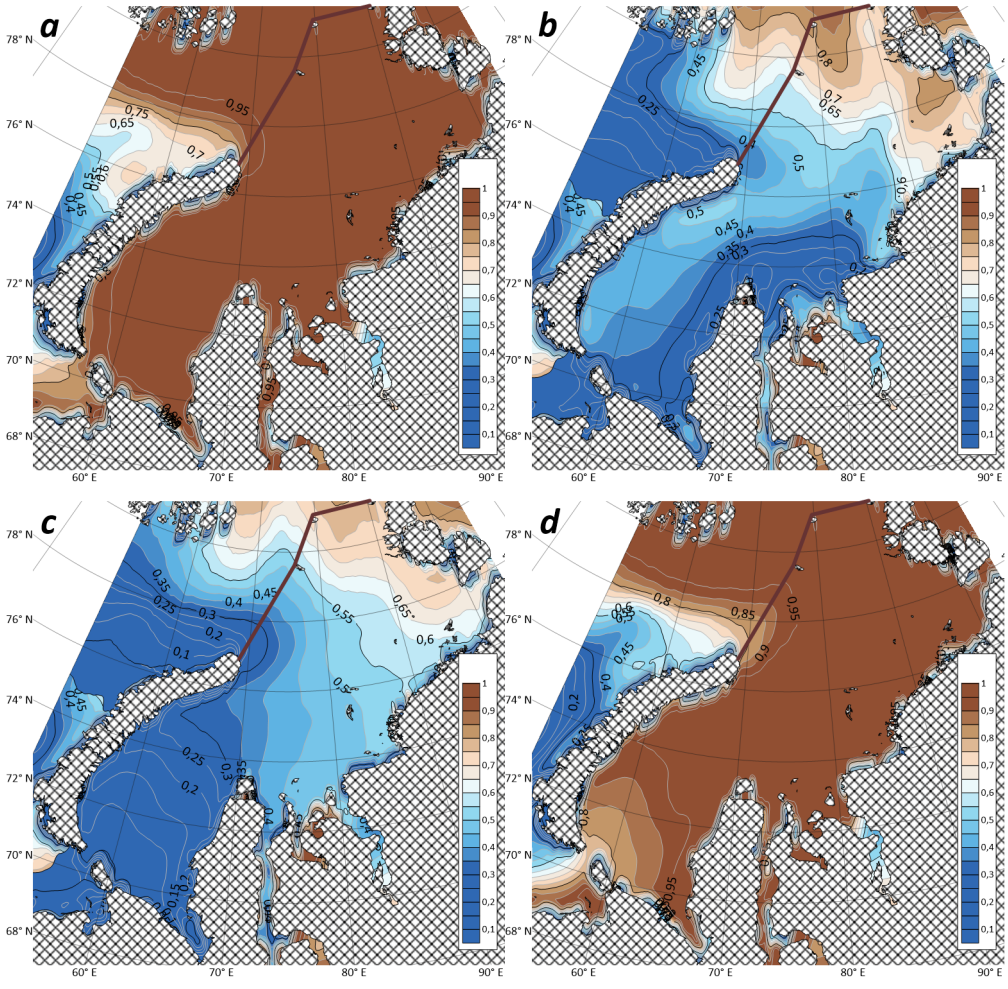

Figure 8. The probability of the presence of ice with a concentration of more than 50% in the Kara Sea according to reanalysis data (in 0–1 unit) for the periods: MAM (a), JJA (b), SON (c), DJF (d).

https://doi.org/10.5194/nhess-2020-198
Preprint. Discussion started: 7 July 2020

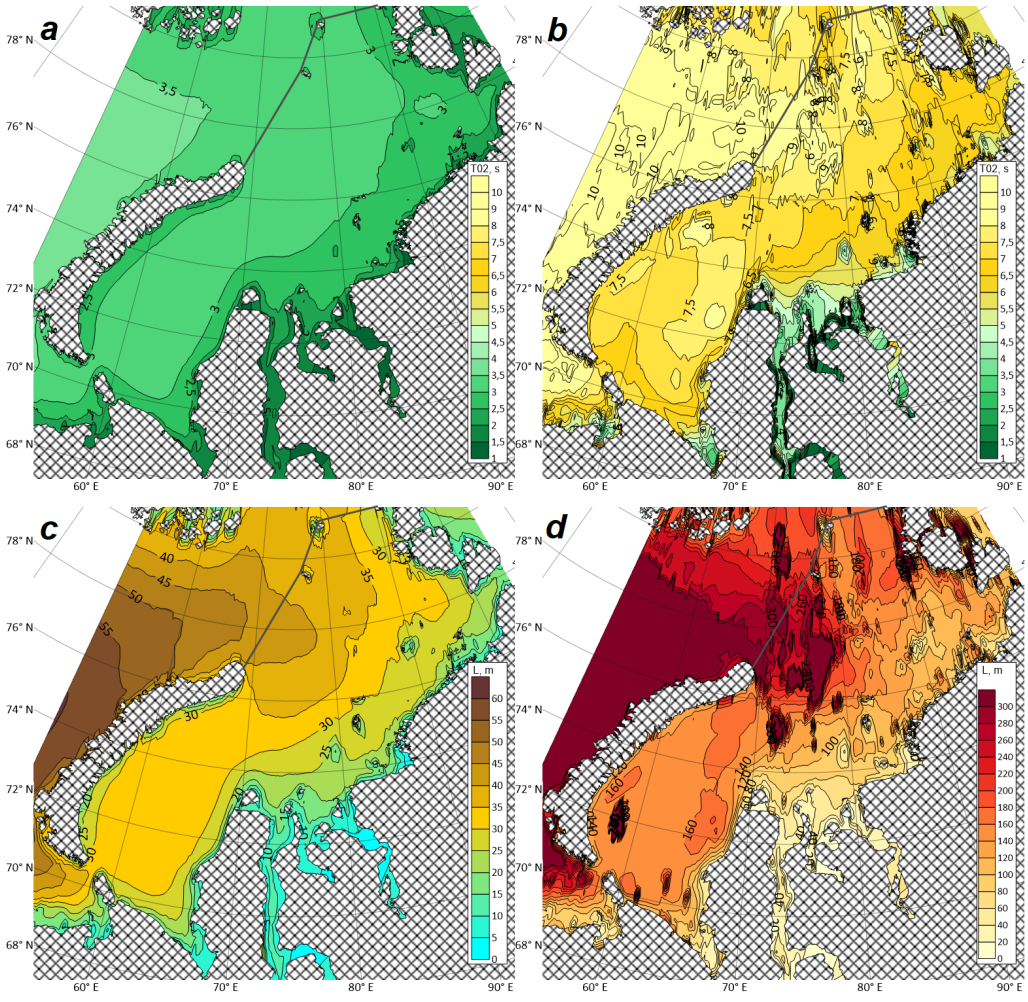

Figure 9. The long-term mean period (a), the maximum period (b), the long-term mean wavelength (c), and the maximum wavelength (d) in the Kara Sea according to modeling data for the period from 1979 to 2017.

https://doi.org/10.5194/nhess-2020-198
Preprint. Discussion started: 7 July 2020

Natural Hazards and Earth System Sciences
Discussions
Open Access
EGU

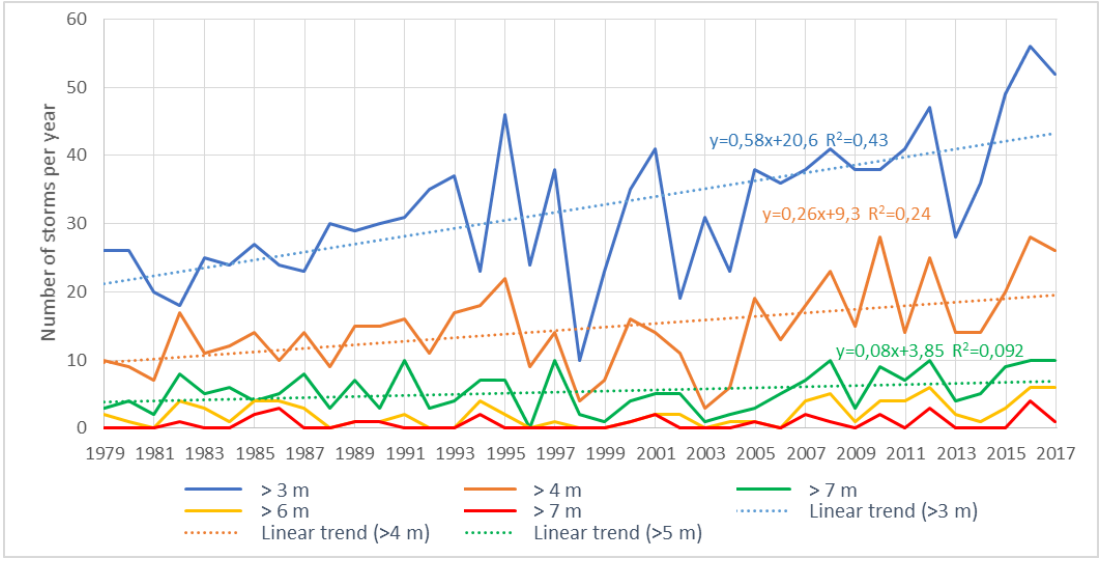

Figure 10. The number of storms with different thresholds per year and its linear trends for 1979 to 2017.

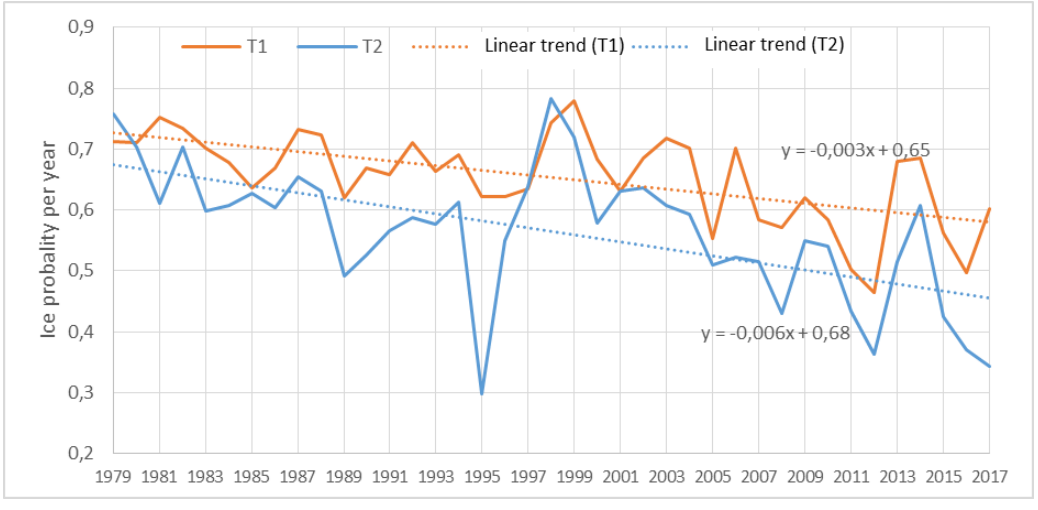

Figure 11. The probability of the ice presence with a concentration of more than 50% for two points in the Kara Sea by years.

https://doi.org/10.5194/nhess-2020-198
Preprint. Discussion started: 7 July 2020

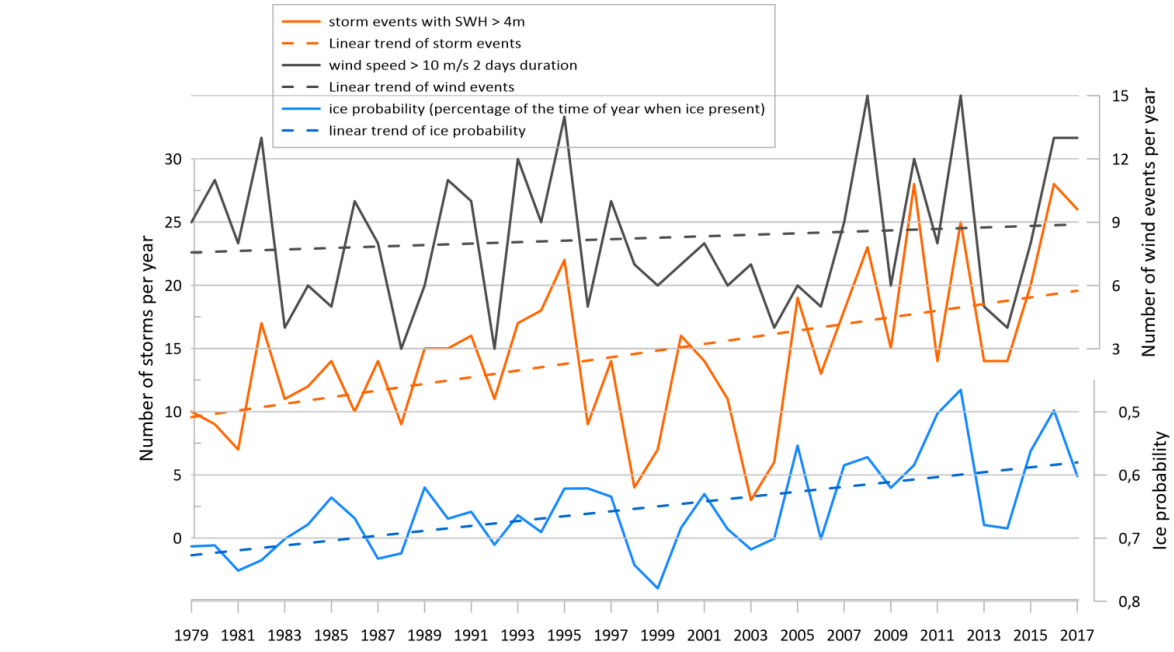

570

571 Figure 12. Recurrence of wind speed of more than 10 m/s and 2 consecutive days at point T1, the number of storms with a
572 threshold 4 m, and probability of the ice presence in point T1(opposite scale).

573

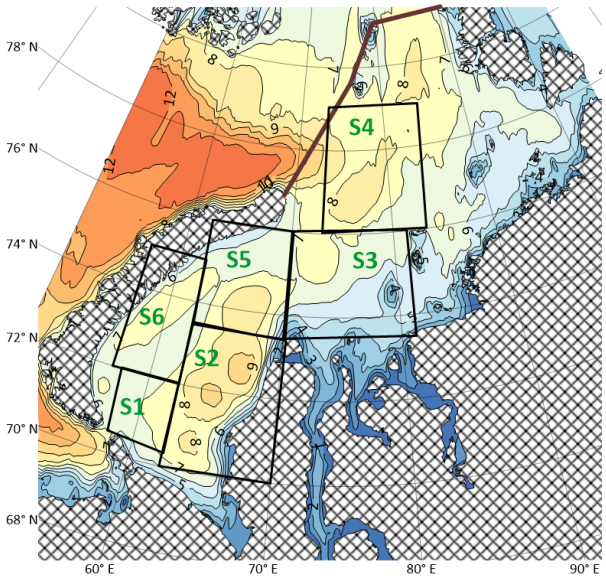

574

575 Figure 13. The SWH maximum and segmentation of the Kara sea: six sectors with different wave conditions.

576

https://doi.org/10.5194/nhess-2020-198
Preprint. Discussion started: 7 July 2020

Natural Hazards and Earth System Sciences
Discussions

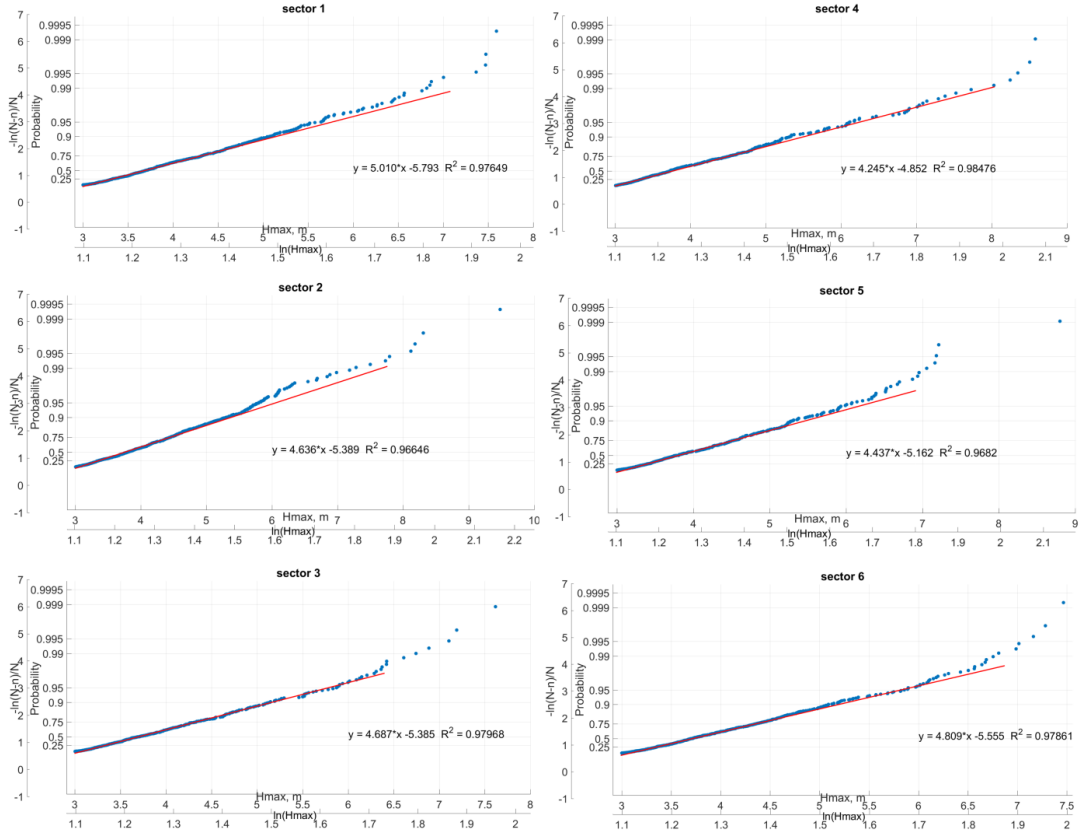

Figure 14. The empirical probability distribution of storms with different wave heights for each of the six sectors, presented in the Pareto logarithmic coordinates. The coefficient of determination and regression equations are given for each sector.

https://doi.org/10.5194/nhess-2020-198
Preprint. Discussion started: 7 July 2020

Natural Hazards and Earth System Sciences
Discussions
Open Access
EGU

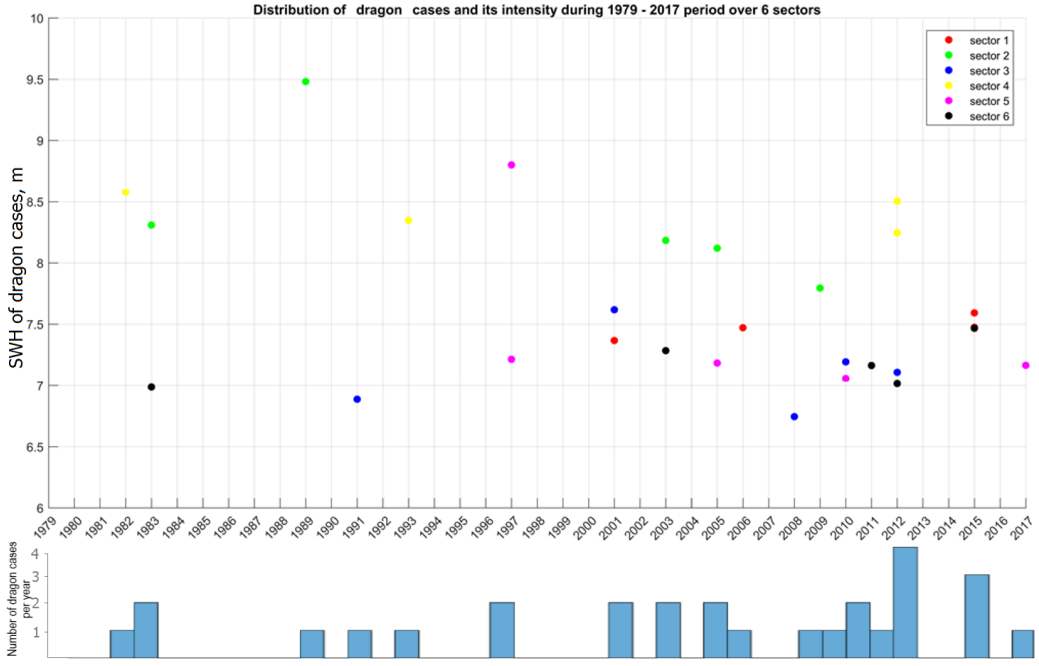

Figure 15. Cases of extreme events (dragons) from 1979 to 2017 for all sectors of the Kara Sea.